◆ Human Brain Mapping 37:4454–4471 (2016) ◆

Brain Dynamics of Post-Task Resting State are Influenced by Expertise: Insights From Baseball Players

Jordan Muraskin,[1]* Sonam Dodhia,[1] Gregory Lieberman,[2,3] Javier O. Garcia,[2] Timothy Verstynen,[4] Jean M. Vettel,[2,3,5] Jason Sherwin,[1] and Paul Sajda[1]*

[1]Department of Biomedical Engineering, Columbia University, New York, New York
[2]U.S. Army Research Laboratory, Human Research and Engineering Directorate, Aberdeen Proving Ground, Aberdeen, Maryland
[3]Department of Bioengineering, University of Pennsylvania, Philadelphia, Pennsylvania
[4]Department of Psychology and Center for the Neural Basis of Cognition, Carnegie Mellon University, Pittsburgh, Pennsylvania
[5]Department of Psychological & Brain Sciences, University of California, Santa Barbara, California

Abstract: Post-task resting state dynamics can be viewed as a task-driven state where behavioral performance is improved through endogenous, non-explicit learning. Tasks that have intrinsic value for individuals are hypothesized to produce post-task resting state dynamics that promote learning. We measured simultaneous fMRI/EEG and DTI in Division-1 collegiate baseball players and compared to a group of controls, examining differences in both functional and structural connectivity. Participants performed a surrogate baseball pitch Go/No-Go task before a resting state scan, and we compared post-task resting state connectivity using a seed-based analysis from the supplementary motor area (SMA), an area whose activity discriminated players and controls in our previous results using this task. Although both groups were equally trained on the task, the experts showed differential activity in their post-task resting state consistent with motor learning. Specifically, we found (1) differences in bilateral SMA–L Insula functional connectivity between experts and controls that may reflect group differences in motor learning, (2) differences in BOLD-alpha oscillation correlations between groups suggests variability in modulatory attention in the post-task state, and (3) group differences between BOLD-beta oscillations that may indicate cognitive processing of motor inhibition. Structural connectivity analysis identified group differences in portions of the functionally derived network, suggesting that functional differences may also partially arise from variability in the underlying white matter pathways. Generally, we find that brain dynamics in the post-task resting state differ as a function of subject expertise and potentially result from differences in both functional and structural connectivity. *Hum Brain Mapp 37:4454–4471, 2016.*

Contract grant sponsor: National Institutes of Health; Contract grant numbers: R01-MH085092, T35-AG044303; Contract grant sponsor: U.S. Army Research Laboratory under Cooperative Agreement Number W911NF-10-2-0022.

*Correspondence to: Jordan Muraskin; Department of Biomedical Engineering, Columbia University, New York, New York. E-mail: jsm2112@columbia.edu; Paul Sajda; E-mail: psajda@columbia.edu

Received for publication 16 February 2016; Revised 7 July 2016; Accepted 8 July 2016.

DOI: 10.1002/hbm.23321

Published online 22 July 2016 in Wiley Online Library (wileyonlinelibrary.com).

Key words: EEG; fMRI; simultaneous; DTI; expertise; baseball; resting-state

INTRODUCTION

The post-task resting state has been described as a "task-driven" functional network state [Wang et al., 2012] associated with learning [Albert et al., 2009; Lewis et al., 2009; Vincent, 2009] and cognition [Grigg and Grady, 2010; Hasson et al., 2009; Waites et al., 2005]. This is premised on the idea that if subjects are interested in improving performance on a task, they may covertly rehearse the task that they just completed, a process which is hypothesized to reengage the task-dependent brain network dynamics just evoked and promote learning and adaption during this rest period. Consequently, it is purported that recruitment of task-related brain dynamics during a post-task resting-state might facilitate the development of expertise in a task over time [Zhang et al., 2014].

To study post-task resting state dynamics, a subject population is often trained on a task and incentivized to perform like experts [Grigg and Grady, 2010; Zhang et al., 2014]. The challenge is that such incentives are rather contrived, using laboratory tasks that have only modest reward/value for the subjects and relying on a few dollars of monetary payout as the incentive. Another approach, the one that we adopt here, is to identify a population that has substantial expertise and intrinsic motivation for a task and have them perform a related surrogate task in the laboratory. In this way, we can tap into robust and real-world brain dynamics, leveraging expertise and inherent value that have been developed in the task over years, to investigate post-task resting state.

While likely facilitated by innate sensorimotor predispositions, such as exceptional visual acuity or motoric agility, it has been proposed that athletes largely develop their cognitive expertise through continued practice and learning [Miura et al., 2010]. As an example, baseball players are exceedingly good at deciding whether to swing at a pitch, given a split second to observe a baseball's trajectory, spin, and speed. During this split second decision, there is little time for explicit decision-making; instead, the ability to hit a baseball relies on largely implicit mechanisms that must link perception to action as a fast perceptual decision [Muraskin et al., in press; Muraskin et al., 2015; Nakamoto and Mori, 2008; Radlo et al., 2001]. This process is largely dependent on the efficiency of globally distributed networks throughout the brain [Forstmann et al., 2010; Heekeren et al., 2004]; however, precisely which functional and structural components of these networks foster expert level performance remains a mystery.

Our goal in the current article is to investigate differences between groups (expert/baseball-hitters vs. novices/controls) in post-task resting state functional networks, where these differences relate to group-level differences in the functional activity assessed during the task. We recruited Division 1 collegiate baseball players as an expert group as well as a matched control group, and we perform a seed-based connectivity analysis. We use seeds in right and left supplementary motor area (SMA) regions, including the preSMA, since we have previously shown in an EEG-only study [Muraskin et al., 2015] and during the task portion of this dataset [Muraskin et al., in press] that task-related differences between baseball players and controls were found in the SMA, and interestingly not in other areas associated with Go/No-Go tasks. A whole brain analysis with respect to these seed regions was performed to investigate group differences in the post-task resting state that may reflect expertise effects with respect to motor learning, modulatory attention, and cognitive processing related to motor inhibition. Together with our previous results, SMA was targeted as a seed region given its known role in motor learning [Aizawa et al., 1991; Halsband and Freund, 1990; Halsband and Lange, 2006; Sakai et al., 1996] and involvement in Go/No-Go tasks [Dunovan et al., 2015; Forstmann et al., 2010; Frank et al., 2015; Jahfari et al., 2012; Simmonds et al., 2008].

In addition to BOLD correlations, we also examined correlations between alpha and beta activity in the SMA and the rest of the brain. Alpha oscillations have been linked with attention-related circuits [Capotosto et al., 2009; Klimesch et al., 1998; Laufs et al., 2003a; Ray and Cole, 1985] and modulation of attention is important for both motor learning [Jueptner et al., 1997; Wulf et al., 2001] and learning in general [Lewis et al., 2009]. Similarly, beta oscillations play a role in cognitive [Ray and Cole, 1985; Wang et al., 2013] and motor processing, especially motor inhibition [Zhang et al., 2008]. The beta wave has been shown to reflect cognition-related processes during rest [Laufs et al., 2003b] and during tasks [Ray and Cole, 1985], with others linking it to involvement in motor activity [Hari and Salmelin, 1997; Kristevafeige et al., 2002]. For example, beta wave synchronization after movement has been described as a marker of an idling motor cortex [Cassim et al., 2001; Pfurtscheller, 1996].

In our experiment, both baseball experts and control participants performed a surrogate pitch discrimination task in a Go/No-Go paradigm [Muraskin et al., in press; Muraskin et al., 2015; Sherwin et al., 2015] while simultaneous fMRI/EEG neuroimaging is collected, and we examined expertise effects in brain dynamics of the post-task resting state as well as related structural connectivity differences from DTI data. We examined three estimates of SMA region activity, that include the pre-SMA, from the averaged fMRI BOLD activity and from EEG sources, including mean alpha and beta power. In each case, we identified relationships between the SMA region seeds and the fMRI functional activity in all voxels outside of the

SMA regions that demonstrated expertise-related effects. Finally, we examined whether expertise differences arose from variation in underlying structural connectivity of the network. Using the ten functionally derived regions of interest from the fMRI/EEG analysis, we compared differences in the number of tracked streamlines between each pair of regions, where differences can be interpreted as the strength of connections [Griffa et al., 2013]. Collectively, this set of analyses assessed whether functional and/or structural connectivity can identify neural correlates of expertise by differentiating expert baseball hitters from controls.

METHODS

Subjects

This study included 14 Division I collegiate Ivy League championship baseball players (all male, 19.57 ± 2.4 years) and 24 non-baseball players (all male, 20.92 ± 2.7 years) with an age range of 18–30 years. None of the non-baseball players (controls) had professional or collegiate baseball experience. Subjects reported no history of neurological problems and had normal or corrected to normal vision. All subjects gave informed consent according to the guidelines and approval of the Columbia University Institutional Review Board.

Behavioral Paradigm

This behavioral paradigm consisted of a Go/No-Go task using simulated baseball pitch videos that have been applied previously [Muraskin et al., 2015; Sherwin et al., 2015]. The task based portion of this experiment is described in Muraskin et al. [in press]. For clarity, we reiterate the experimental procedure below. The experiment involved a training session prior to the simultaneous fMRI/EEG data acquisition. During training, subjects familiarized themselves with the different pitch types and completed practice trials until they have scored an accuracy of at least 60% (above the random chance accuracy of 50%).

At the beginning of each trial, a single letter corresponding to the pitch ("F" for fastball, "C" for curveball, and "S" for slider) was shown on the screen (horizontal view 0.28°and vertical view 0.28°) for a mean time of 819 ± 3.1 ms. While the letter was on the screen, a horizontal bar (horizontal extent 3.93°, vertical 0.28°) shrank (horizontally) at a constant rate to either the left or right side of the screen. If the pitch following the letter cue came from a left handed pitcher, then the horizontal bar shrank toward the right, and if the pitch came from a right handed pitcher, then the horizontal bar shrank toward the left. After the horizontal bar shrank completely to either the left or the right, the pitch started from that point on the left or right side of the screen (i.e., pitches from left-handed pitchers started from the right side of the screen, and vice versa).

Subjects used the VisuaStim Digital System (Resonance Technology) 600x800 goggle display to view 450 simulated baseball pitches (5 blocks of 90 trials, 3 different types of pitches) from the viewpoint of a baseball catcher (at the end of the baseball's trajectory). While viewing these pitches, subjects completed a Go/No-Go task by determining if each pitch matched its pre-stimulus cue. The program optseq2 [Dale, 1999] was used to select a mean jittered inter-stimulus interval (ISI) that enabled the rapid presentation of fMRI events without overlap from the hemodynamic responses (mean of 3,000 ms and SE of 225 ms). Each subject was instructed to respond by pressing a keyboard button with the index finger of his right hand if the pre-stimulus cue matched the type of pitch that followed it ("Go" trials). In addition, in order for a "Go" response to be correct, the subject needed to respond while the ball was still in the screen. If the pre-stimulus cue and the pitch did not match, the subject was instructed to withhold his response ("No-Go" trials). Feedback was given after every trial (for both "Go" and "No-Go" trials) in the form of a "+" for correct responses in "Go" trials and correct withholding of responses in "No-Go" trials and a "−" for incorrect "Go" and "No-Go" responses. Sixty percent of the trials were "Go" and 40% of the trials were "No-Go."

Overall accuracy on the task was determined by calculating the percent of trials with a correct response (the subject responded while the ball was still on the screen for "Go" trials and withheld his response for "No-Go" trials). Go accuracy was determined by calculating what percent of all the "Go" trials had a correct response (subject responded and this response happened while the ball was still on the screen). "No-Go" accuracy was determined by calculating what percent of all the "No-Go" trials the subject correctly withheld his response.

Pitch Simulations

Following our previous work [Muraskin et al., in press; Muraskin et al., 2015; Sherwin et al., 2012, 2015], the pitch simulations were created by solving six-coupled differential equations [Adair, 1990; Armenti, 1992] in MATLAB 2010a (Mathworks, Natick, MA) using a differential equation solver. The PsychToolbox [Brainard, 1997; Pelli, 1997] was used to present the simulated baseball pitches. In the pitch simulations, an isoluminant green circle moving in the plane of the screen represented a baseball pitch, and it simulated movement in the plane perpendicular to the screen (depth) by increasing in size while approaching the subject.

Three different pitch categories (fastball, curveball, and slider) were used in this paradigm, and these pitches were identified by their trajectory only (even though these pitches also have spin in real-life). A fastball has a

trajectory that is straight, a curveball has a combination of side and top spin that takes the ball on a rightward and downward trajectory, and a slider only has side spin that takes it on a rightward trajectory [Sherwin et al., 2012].

$$\frac{dx}{dt} = v_x \quad (1)$$

$$\frac{dy}{dt} = v_y \quad (2)$$

$$\frac{dz}{dt} = v_z \quad (3)$$

$$\frac{dv_x}{dt} = -F(v)vv_x + B\omega(v_z \sin\Theta - v_y \cos\Theta) \quad (4)$$

$$\frac{dv_y}{dt} = -F(v)vv_y + B\omega v_y \cos\Theta \quad (5)$$

$$\frac{dv_z}{dt} = -g - F(v)vv_z + B\omega v_x \sin\Theta \quad (6)$$

$$F(v) = 0.0039 + \frac{0.0058}{1 + e^{\frac{(v - v_d)}{\Delta}}} \quad (7)$$

The first three equations specify the change in spatial location in each direction,which equals the velocity of the baseball. Equations 4–6 specify the accelerations due to the drag [$F(v)$], the Magnus force (B), and gravity (g) acting on the baseball. Equation 7 is used to calculate the drag force at different velocities with $v_d = 35$ m/s and $\Delta = 5$ m/s. The Magnus force (B), which occurs due to differential drag on a spinning object, is approximated here to be 4.1×10^{-4} (dimensionless). After specifying the initial conditions [x_0, y_0, z_0, v_{x0}, v_{y0}, v_{z0}, ω (rotational frequency)], the six ordinary differential equations were solved in MATLAB. Each of the three pitch categories have well-defined ranges of initial velocities and rotation angles, and within these ranges, pitches were varied so that no two trials of the same category had the exact same trajectory.

fMRI/EEG Resting State Scan

After completing the Go/No-Go perceptual decision-making task, participants waited about 2 minutes while the MRI technician prepared the scanner for the final 5 minute resting state scan. Participants were told to "rest and focus on the cross on the screen," and they rested supine in the MRI scanner with eyes open and fixated on a central point.

Simultaneous fMRI/EEG and DTI Data Acquisition

A 3T Philips Achieva MRI scanner (Philips Medical Systems) with an eight channel SENSE head coil was used to collect MRI data. Functional echo planar imaging (EPI) data sensitive to blood oxygenated level-dependent (BOLD) contrast were collected (2 s TR, 20 ms TE, 64 × 64 matrix, and 35 interleaved slices). Whole brain T1-weighted anatomical images (1 × 1 × 1 mm) and single high volume EPI images (2 × 2 × 2 mm) were also obtained to help with registration. DTI was acquired along 50 directions with a b-value of 1,500 s/mm^2 (as well as a b0 image with no diffusion weighting) and a voxel-size of 2 × 2 × 2 mm^3 (TR = 8,996 ms, TE = 80 ms, FOV = 224 mm, 75 axial slices AC/PC aligned encompassing the whole brain, SENSE Factor = 2).

Simultaneous and continuous EEG data were acquired with a custom built MR-compatible EEG system [Goldman et al., 2009; Sajda et al., 2010]. This system included a differential amplifier and a bipolar EEG cap with 36 Ag/AgCl electrodes (including left and right mastoids) arranged as 43 bipolar pairs. In order to minimize noise from subject head motion in the main magnetic field and from inductive pickup from magnetic gradient pulses, we used twisted bipolar pair leads. The 488 Hz sampled EEG was synchronized with the scanner clock at the start of each functional image acquisition by sending a transistor–-transistor logic (TTL) pulse to the recording computer. This was used in the gradient artifact removal during the offline EEG data preprocessing steps. About 10 kΩ resistors were built into each electrode to ensure subject safety, and all electrode impedances were kept below 20 kΩ.

fMRI/EEG Data Preprocessing

Simultaneous fMRI/EEG data collection introduces some known confounds (i.e., gradient and ballistocardiogram artifacts (BCG) in EEG and bias field distortion in fMRI) that were removed with standard EEG/fMRI processing [Walz et al., 2013], and then each neuroimaging modality was preprocessed according to well-adopted approaches for its imaging type. Based on previous findings in EEG-only [Muraskin et al., 2015] and the task based EEG-fMRI [Muraskin et al., in press] studies that highlight SMA involvement in Go/No-Go tasks with expertise, our analysis focused on connectivity relationships between R and L SMA functional activity, either fMRI or EEG, and the fMRI activity in all voxels located outside of the SMA. Consequently, each preprocessing stream targeted an end state that produced a representative time series for the SMA by either averaging voxels in the fMRI data or by estimating a dipole source in the EEG data.

fMRI preprocessing

SPM8 (Wellcome Trust Centre for Neuroimaging, London) was used to preprocess the resting state fMRI EPI images (bias field correction, slice-time correction, motion realignment, normalization, and smoothing) and MPRAGE structural images (segmentation and normalization). The realignment parameters from the motion realignment step were included as first level covariates in the fMRI analysis. In a segmentation step, a mask for each subject's gray matter, white matter, and CSF images were obtained, and a group gray matter mask (size 199,768 voxels; 1 voxel = 2 × 2 × 2 mm^3) was created by averaging the gray matter

images from all of the subjects. This mask was used as input into the Functional Connectivity (CONN) toolbox [Whitfield-Gabrieli and Nieto-Castanon, 2012] to ensure that all the ROIs detected in the seed to voxel connectivity analysis were in the brain's gray matter. Furthermore, using CONN's anatomical aCompCor strategy, noise signals due to CSF, white matter, realignment parameters, and time-series predictors of global signal were removed [Behzadi et al., 2007]. Finally, the AAL atlas [Tzourio-Mazoyer et al., 2002] was used on the MPRAGE image to parcellate the gray matter voxels into regions, and the voxels within the SMA were averaged to produce a functional fMRI time series for the connectivity seed analysis.

EEG preprocessing

Matlab (Mathworks, Natick, MA) was used to preprocess the resting state EEG data. First, gradient artifact removal was performed using a template subtraction algorithm [Goldman et al., 2009]. Then, a software-based 0.5 Hz high pass filter was used to remove DC drifts, a 60 Hz (harmonic) notch filter to minimize line noise artifacts, and a 100 Hz low pass filter were applied before resampling the data to 256 Hz. These filters were designed to be zero-phase to minimize delay distortions. Independent components analysis (ICA) was run using EEGLAB [Delorme and Makeig, 2004] and the FastICA [Hyvarinen, 1999] algorithm was used to remove eye-blink artifacts. This methodology has been used previously to identify and remove eye-blink artifacts reliably [Muraskin et al., 2015; Sherwin et al., 2012; Sherwin and Sajda, 2013]. Stimulus events—that is, countdown, pitch type, responses—were recorded on separate channels for event-related analysis.

Ballistocardiogram artifacts are more challenging to remove because they share frequency content with EEG activity. BCG artifacts were removed from the continuous gradient-free data using a principal components analysis method [Goldman et al., 2009; Sajda et al., 2010]. First, the data were low passed at 4 Hz to extract the signal within the frequency range in which BCG artifacts are observed and then the first two principal components were determined. The channel weightings corresponding to those components were projected onto the broadband data and subtracted out. These BCG-free data were then re-referenced from the 43 bipolar channels to the 34-electrode space.

We performed cortical source imaging using eConnectome [He et al., 2011]. eConnectome uses the cortical current density source model to solve the inverse problem in order to determine cortical source distribution. After producing a high resolution cortical surface, it down-samples the cortical surface to 7,850 current dipoles spread evenly across and perpendicular to the cortical surface. The dipole strengths on the cortical surface were estimated, and using the region of interests defined by the AAL atlas, the dipole located in R and L SMA was identified. A Morlet transformation was applied to the SMA time series in order to obtain a power-time series. The power corresponding to alpha (8–12 Hz) and beta (15–30 Hz) waves was normalized by dividing the power at each time point by the mean power. The EEG data (8–12 Hz and 15–30 Hz) were then convolved with a canonical hemodynamic response function so that it modeled blood oxygen level dependent (BOLD) changes. An average value was obtained for every 2-s interval for the alpha (8–12 Hz) and beta (15–30 Hz) power time courses.

Seed to Voxel Connectivity Analysis

Our analysis focused on connectivity relationships between R and L SMA seed regions and all fMRI voxels outside of the SMA that are located in the brain's gray matter. We either averaged the fMRI time series across all SMA voxels to produce the seed time series, or we estimated the EEG source time series for a dipole located near the SMA region. The SMA time series, either fMRI or EEG, was then used in a regression with all non-SMA fMRI voxels. A flow chart of the processing stream is detailed in Figure 1.

For each subject, we created a regression contrast image for three SMA time series: the first uses fMRI SMA time series data, the second uses EEG alpha (8–12 Hz) SMA data controlling for the fMRI SMA time series, and the third uses EEG beta (15–30 Hz) SMA data controlling for the fMRI SMA time series. These individual contrasts were done separately for R and L SMA and then used in two group analyses. The first group general linear model (GLM) investigated expertise effects, directly comparing the baseball experts and controls. The second group GLM examined connectivity relationships with overall accuracy on the Go/No-Go task while controlling for expertise by including group assignment as a regressor in the GLM (1 for expert and 0 for control). Thus, the second group analysis identified fMRI voxels that varied with R or L SMA activity (fMRI, EEG alpha, or EEG beta) based on the person's task performance, independent of their expertise. We also ran one variant of the second group analysis, using the participant's performance accuracy on only the "No-Go" trials and the EEG beta SMA activity based on prior evidence of beta power involvement in motor response inhibition [Zhang et al., 2008].

We generated a regression contrast image for each group analysis. To minimize type I and type II errors, we used AFNI's 3dClustSim program to determine a FWE-corrected P value <0.05. The group gray matter mask (199,768 voxels) was used as input for a Monte Carlo simulation (10,000 iterations) with parameters for set for voxel size ($2 \times 2 \times 2$) and smoothing (FWHM 8 mm), and we found that our uncorrected P value and minimum cluster size threshold for significance was $P < 0.005$ (uncorrected) and a minimum cluster size of 156 voxels.

For each region of interest (ROI) cluster that reached significance, we extracted parameter estimates/β weights (measure of functional connectivity strength in arbitrary units) for each subject, then conducted post-hoc independent samples t-tests and plotted average functional

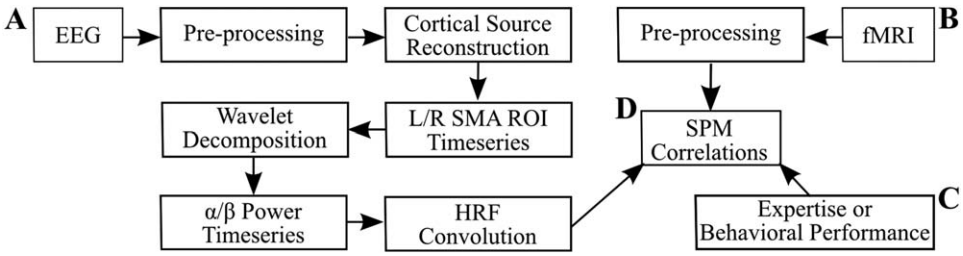

Figure 1.

Resting-state FMRI/EEG methods diagram. A, EEG data were first preprocessed by removing gradient artifacts, then filtered, down-sampled, BCG removed, and re-referenced to 34-electrode space. Dipole strengths on the cortical surface were then estimated and averaged at both L and R SMA. A Morlet transformation was applied to the time series to generate α and β power fluctuations across time. Finally, the α and β power time series were convolved with the canonical hemodynamic response function (HRF). B, Preprocessing was done on the fMRI data (slice-time correction, motion realignment, normalization, and smoothing) and MPRAGE structural images (segmentation and normalization). Filtered BOLD time courses from L and R SMA regions were averaged to be seed regions for further analysis. C, Covariates of interest were created either by the grouping of subjects by expertise or creating continuous regressors based on each subject's task performance. D, A seed to voxel connectivity analysis was performed between L and R SMA seed regions (fMRI voxels or α and β power source time series) and the gray matter voxels outside of L and R SMA. Statistical parametric maps were created by analyzing group differences or correlating subject performance with seed to voxel connectivity.

connectivity parameter (and standard error) in each group to show the strength of the functional connectivity in each of the groups. We also conducted post-hoc Pearson correlation coefficient analyses between connectivity parameters to examine the direction of the relationship, where positive values indicate that the task performance increased and negative values are related to decreases in performance.

Structural Connectivity Analysis

Structural connectivity was computed using DSI Studio and analyzed using Matlab. First, DTI data were reconstructed using Q-Space Diffeomorphic Reconstruction (QSDR; [Yeh and Tseng, 2011]. Whole-brain fiber tractography [Yeh et al., 2013] was performed 1,000 times for each participant (13 experts, 24 novices, since one expert was excluded for poor normalization into MNI QA space). In order to minimize the impact of local microarchitectural variability on streamline generation, the 1,000 iterations randomly sampled values for QA thresholds (between 0.01 and 0.10), turning angle thresholds (between 40° and 80°), and smoothing (between 50% and 80%) to ensure results are robust to these parameter choices, while using constant values for step size (1 mm) and min/max fiber lengths (10 mm/400 mm). This was done in order for the structural connectivity results to not be biased by a particular parameter scheme, but instead reflect the likelihood of a particular connectivity pattern across parameter dependencies. Each iteration generated 250,000 streamlines, and with a fixed streamline count, differences in the number of estimated fiber tracts can be interpreted as differences in the strength of connection [Griffa et al., 2013].

A targeted ROI analysis was performed on the ten functionally derived regions of interest from the fMRI/EEG expert versus novice analysis: L insula, L superior frontal gyrus (SFG), L superior parietal cortex, L posterior cingulate gyrus, R SFG, R inferior frontal gyrus (IFG), R precentral gyrus, R superior parietal gyrus, R middle temporal gyrus, R cerebellum. The fMRI/EEG seed regions in L and R supplementary motor areas (SMA) from the AAL atlas were also included. Visual inspection confirmed that these masks subsumed most of the preSMA as well [Zhang et al., 2012]. To determine the strength of structural connections, the numbers of streamlines passing through each region-pair were averaged across iterations, and type two *t*-tests were performed to compare expertise-related structural connectivity patterns between experts and novices.

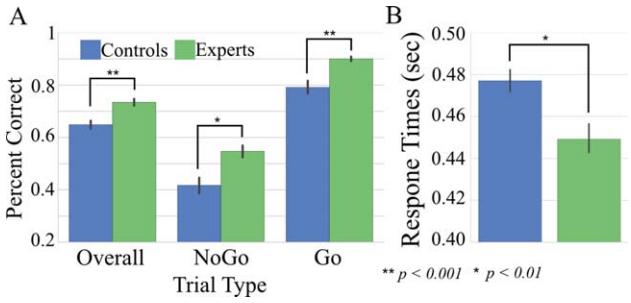

Figure 2.

Behavioral results for Go/No-Go task. A, Behavioral task accuracy for the task overall and then split by No-Go and Go trial accuracy. Two-way independent t-tests were used to test for significant differences between groups. B, Average response times for correct Go trials split by expertise group. [Color figure can be viewed at wileyonlinelibrary.com]

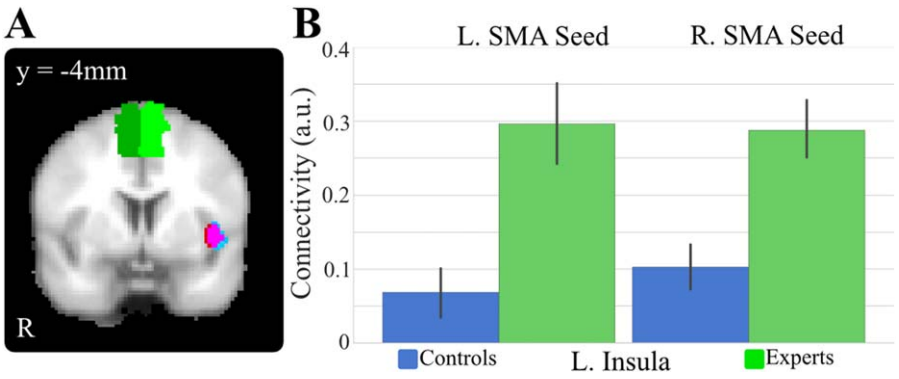

Figure 3.

Expertise differences in the functional connectivity to SMA. A, Overlay of the functional connectivity differences at L insula between experts and controls to R SMA (red), L SMA (blue), and overlap (magenta). B, Post-hoc tests show significant differences between the two groups, with experts having a significantly higher connectivity to L and R SMA at L insula. [Color figure can be viewed at wileyonlinelibrary.com]

RESULTS

Behavioral Results

Behavioral task results are shown in Figure 2. Overall accuracy (% correct trials) for controls was 65% ± 8 and for experts was 73% ± 5. Experts had significantly higher accuracy compared with controls ($t = 4.16$, $P = 0.0002$, Cohen's $d = 1.33$). Expert No-Go (55% ± 9) and Go trial (90% ± 3) accuracies were significantly higher than the control group (42% ± 15, 79% ± 13) (No-Go Trials: $t = 3.31$, $P = 0.0021$, Cohen's $d = 1.04$; Go Trials: $t = 3.86$, $P = 0.006$, Cohen's $d = 1.14$). Experts (449 ± 24 ms) also have faster reaction times than controls (477 ± 25 ms) for Correct Go trials ($t = -3.24$, $P = 0.0031$, Cohen's $d = -1.09$).

Group Analysis: Expert Versus Control

A significant group effect was found in resting state functional connectivity between the R SMA (AAL atlas) and the L insula (MNI peak [−42 10 −8], $t = 3.84$, $Z = 3.49$, $P < 0.001$; cluster volume of 1,920 mm^3). Post-hoc t-tests revealed that experts had

TABLE I. fMRI Only: Seed-based post-task resting state functional connectivity of R and L SMA voxels with the rest of the brain's gray matter voxels

Seed	Contrast	Region name	MNI coordinates X	Y	Z	Voxels	T-score	Z-score
fMRI BOLD at R. SMA	**Experts > Non-experts**	L insula	−42	10	−8	240	3.84	3.49
	Non-experts > Experts	(None)						
fMRI BOLD at L. SMA	**Experts > Non-experts**	L insula	−44	6	−6	276	3.68	3.37
	Non-experts > Experts	(None)						
fMRI BOLD at R. SMA	**Overall Accuracy Regressor,**	R. insula	42	−18	−14	261	4.88	4.23
	Controlling for Expertise	R superior frontal gyrus	24	44	34	194	4.41	3.91
	Positive Correlations							
	Overall Accuracy Regressor,	L Parahippocampal	−24	−14	−30	160	4.08	3.66
	Controlling for Expertise							
	Negative Correlations							
fMRI BOLD at L. SMA	**Overall Accuracy Regressor,**	R insula	42	−14	0	307	3.97	3.58
	Controlling for Expertise							
	Positive Correlations							
	Overall Accuracy Regressor,	L Cerebellum	−28	−48	−26	220	4.68	4.10
	Controlling for Expertise							
	Negative Correlations							

Reports all clusters with uncorrected $P < 0.005$ and minimum cluster extent threshold (contiguous voxels) 156 voxels.

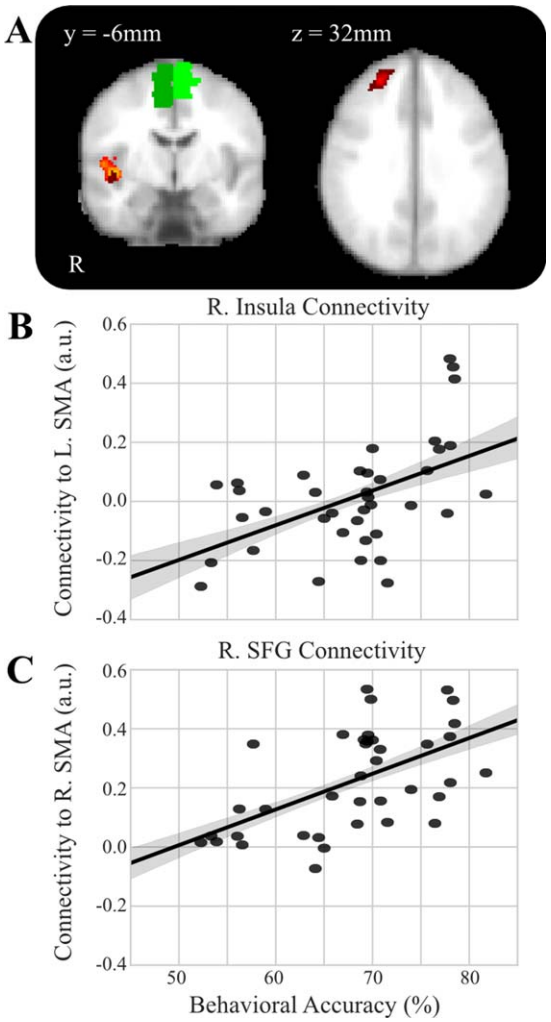

Figure 4.

SMA functional connectivity correlates with task performance. A, Overlay of significant clusters where task performance correlates with functional connectivity to L SMA (orange) and R SMA (dark red). B, Scatter plot of the functional connectivity to L SMA from R insula by the behavioral accuracy of each subject controlling for expertise ($r = 0.509$, P value $= 0.001$). C, Scatter plot of the functional connectivity to R SMA from R SFG by the behavioral accuracy of each subject controlling for expertise ($r = 0.56$, P value < 0.001). [Color figure can be viewed at wileyonlinelibrary.com]

higher functioned connectivity between the R SMA and the L insula than controls ($t = 3.74$, $P < 0.001$) (Fig. 3A and Table I).

Similarly, a significant group effect in functional connectivity (Fig. 3B) was also found between the L SMA (AAL atlas) and the L insula (MNI peak [−44 6 −6], $t = 3.68$, $Z = 3.37$; $P < 0.001$, cluster volume 2,208 mm^3). Post-hoc *t*-tests revealed that experts had significantly higher functional connectivity than controls ($t = 3.66$, $P < 0.001$).

Group Analysis: Go/No-Go Performance with fMRI SMA

Given the dominance of expertise in the group fMRI-only seed analysis, we added a regressor for expertise level (expert or non-expert) and examined how functional connectivity fluctuated with task performance when using

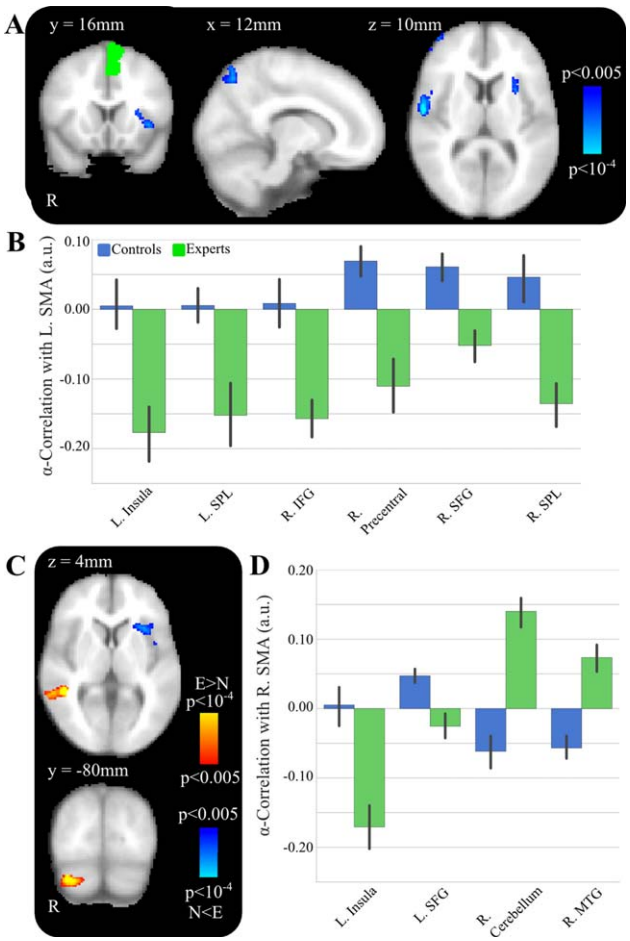

Figure 5.

SMA α power correlations differences between experts and controls. A, Group-level activations for L SMA α-power correlations contrast for controls > experts. Multiple significant clusters are displayed including L insula. B, Post-hoc tests show significant differences between the two groups, with experts having a significantly lower α-connectivity to L SMA at multiple regions. C, Group-level activations for R SMA α-power correlations contrast for controls > experts (blue) and experts > controls (red). Multiple significant clusters are displayed including L insula and R middle temporal gyrus. D, Post-hoc tests show significant differences between the two groups, with experts having a significantly lower α-connectivity to R SMA in L insula and L superior frontal gyrus and significantly higher α-connectivity in R cerebellum and R middle temporal gyrus. [Color figure can be viewed at wileyonlinelibrary.com]

TABLE II. Simultaneous fMRI/EEG Alpha Power: Seed-based post-task resting state functional connectivity of EEG alpha power using R and L SMA sources with all fMRI gray matter voxels outside of R and L SMA

Seed	Contrast	Region name	MNI coordinates			Voxels	*T*-score	*Z*-score
			X	*Y*	*Z*			
EEG Alpha power at R. SMA *Controlling for fMRI signal at R. SMA*	**Experts > Non-experts**	R cerebellum	28	−88	−36	493	5.66	4.76
		R middle temporal gyrus	46	−42	0	442	5.26	4.50
	Non-experts > Experts	L superior frontal gyrus	−22	2	46	328	4.16	3.74
		L insula	−36	16	0	295	3.92	3.56
EEG Alpha Power at L. SMA *Controlling for fMRI signal at L. SMA*	**Experts > Non-experts**	(None)						
	Non-experts > Experts	R precentral	58	−8	14	239	5.04	4.36
		R superior parietal	22	−64	54	374	4.09	3.68
		R superior frontal gyrus	32	52	36	187	3.97	3.59
		R inferior frontal gyrus	52	30	0	197	3.86	3.51
		L insula	−28	20	6	164	3.66	3.35
		L superior parietal	−20	−60	66	184	3.48	3.21

fMRI activity from the R and L SMA as seed regions in separate analyses. Across all subjects, functional connectivity between L SMA was found (Fig. 4A and Table I) to vary positively with task performance (overall accuracy) with R insula (MNI peak [42 −14 0], $t = 3.97$, $Z = 3.58$, $P < 0.001$; cluster volume 2,456 mm^3). Conversely, functional connectivity between L SMA varied negatively with L cerebellum (MNI peak [−28 −48 −26], $t = 4.68$, $Z = 4.10$; $P < 0.001$, cluster volume 1,760 mm^3). When we looked across hemispheres and used the R SMA as the seed region, we found that functional connectivity varied positively according to task performance between R SMA and R insula (MNI peak [42 −18 −14], $t = 4.88$, $Z = 4.23$, $P < 0.001$; cluster volume 2,088 mm^3) and with R superior frontal gyrus (MNI peak [24 44 34], $t = 4.41$, $Z = 3.91$, $P < 0.001$; cluster volume 1,552 mm^3) and negatively between R SMA and L parahippocampal gyrus (MNI peak [−24 −14 30], $t = 4.08$, $Z = 3.66$, $P < 0.001$; cluster volume 1,280 mm^3).

Pearson coefficient correlation tests revealed (Fig. 4B,C) that functional connectivity was positively correlated with overall accuracy scores in the Go/No-Go task for R SMA–R SFG ($r = 0.56$, P value < 0.001), R SMA–R insula ($r = 0.36$, P value $= 0.03$), and L SMA–R insula ($r = 0.509$, P value $= 0.001$), while negatively correlating with overall accuracy scores for R SMA–L parahippocampal ($r = -0.36$, $P = 0.026$) and L SMA–L cerebellum ($r = -0.57$, $P < 0.001$).

Group Analysis: Go/No-Go Performance with EEG Alpha SMA

Next, we used a time series of EEG alpha power from a L SMA EEG source as the seed to examine connectivity relationships with BOLD time series in non-SMA voxels. As shown in Figure 5A and Table II, group differences in correlation were found between the EEG alpha power at L SMA and fMRI BOLD signal at R precentral gyrus (MNI peak [58 −8 14], $t = 5.04$, $Z = 4.36$, $P < 0.001$; cluster volume 1,912 mm^3), R superior parietal gyrus (MNI peak [22 −64 54], $t = 4.09$, $Z = 3.68$, $P < 0.001$; cluster size = 2,992 mm^3), R superior frontal gyrus (MNI peak [32 52 36], $t = 3.97$, $Z = 3.59$, $P < 0.001$; cluster volume 1,496 mm^3), R inferior frontal gyrus (MNI peak [52 30 0], $t = 3.86$, $Z = 3.51$, $P < 0.001$; cluster volume 1,576 mm^3), L insula (MNI peak [−28, 20, 6], $t = 3.66$, $Z = 3.35$, $P < 0.001$; cluster volume 1,312 mm^3), and L superior parietal (MNI peak [−20 −60 66], $t = 3.48$, $Z = 3.21$, $P < 0.001$; cluster volume 1,472 mm^3).

In Figure 5B, post-hoc tests revealed that there were negative correlations in experts and positive correlations in controls between the EEG alpha power for L SMA–R superior parietal fMRI BOLD ($t = 3.61$, $P < 0.001$) and L SMA–R superior frontal gyrus ($t = 3.54$, $P < 0.001$). Post-hoc test revealed that there were negative correlations in experts and negligible correlations in controls between the EEG alpha power at L SMA and the fMRI BOLD signal at R inferior frontal gyrus ($t = 3.45$, $P = 0.001$), L insula ($t = 3.29$, $P = 0.002$), and L superior parietal ($t = 3.24$, $P = 0.003$).

We next examined functional connectivity using EEG alpha power from a R SMA EEG source as the seed region and BOLD time series from non-SMA voxels. As shown in Figure 5C, we found significant group effects. Controls had significantly greater correlation between R SMA and L superior frontal gyrus (MNI peak [−22 2 46], $t = 4.16$, $Z = 3.74$; $P < 0.001$, cluster volume 2,624 mm^3) and L insula (MNI peak [−36 16 0], $t = 3.92$, $Z = 3.56$, $P < 0.001$; cluster volume 2,360 mm^3). Experts had greater correlation between R SMA and R middle temporal gyrus (MNI peak [46 −42 0], $t = 5.26$, $Z = 4.50$, $P < 0.001$; cluster volume 3,944 mm^3).

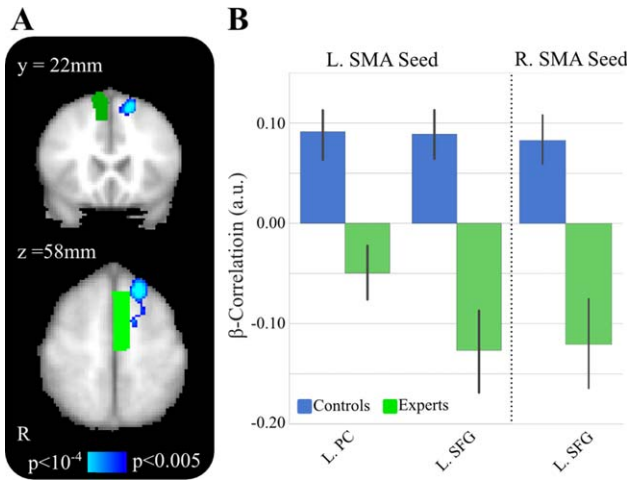

Figure 6.

SMA β power correlations differences between experts and controls. A, Group-level activations for L SMA (bright green) and R SMA (dark green) β-power correlations contrast for controls > experts. B, Post-hoc tests show significant differences between the two groups, with controls having a significantly higher connectivity to L and R SMA at L. superior frontal gyrus. [Color figure can be viewed at wileyonlinelibrary.com]

As shown in Figure 5D, post-hoc *t*-tests revealed that there are strong negative correlations in experts, but negligible correlations in controls between R SMA alpha and L insula ($t = 3.75$, $P < 0.001$). Post-hoc *t*-tests revealed that there were inverse correlations in experts, but positive correlations in controls between R SMA alpha and L superior frontal gyrus ($t = 3.75$, $P < 0.001$). Post-hoc t tests revealed positive correlations in experts and negative correlations in controls between R SMA alpha and R middle temporal gyrus ($t = 4.10$, $P < 0.001$).

Group Analysis: Go/No-Go Performance with EEG Beta SMA

As a complement to the alpha analysis, we implemented the same approach but used beta power. As shown in Figure 6 and Table III, significant group differences were found between the L SMA source seed and L superior frontal gyrus (MNI peak [−18 26 60], $t = 4.99$, $Z = 4.32$, $P < 0.001$; cluster volume 2,416 mm^3) and L posterior cingulum (MNI peak [−8 −42 10], $t = 3.82$, $Z = 3.47$, $P < 0.001$; 1,912 mm^3).

Investigating the R SMA source seed as shown in Figure 6 and Table III, significant group difference were found with fMRI BOLD signal at L superior frontal gyrus (MNI peak [−16 26 58], $t = 4.52$, $Z = 4.00$; $P < 0.001$, cluster volume 1,608 mm^3). Post-hoc tests revealed that the correlation was inverse in experts but positive in controls ($t = 4.23$, $P < 0.001$).

As shown in Figure 7, post-hoc Pearson coefficient correlation tests revealed significant positive correlations between R SMA beta and R parahippocampal gyrus (PHG) ($r = 0.39$, $P = 0.026$) and negative correlations with L SFG ($r = -0.59$, $P < 0.001$) and L anterior cingulate cortex (ACC) ($r = -0.61$, $P < 0.001$). There were no significant correlations with the "No-Go" accuracy using the L SMA beta activity as the seed.

Structural Connectivity Results

Our final analysis used DTI to investigate structural connectivity that may underlie these functional network differences in post-task resting state dynamics between experts and the control group. A targeted ROI analysis was performed on the ten functionally derived regions of interest from the fMRI/EEG analysis, shown in Figure 8A (black orbs): L insula, L superior frontal gyrus, L superior parietal cortex, L posterior cingulate gyrus, R superior frontal gyrus, R inferior frontal gyrus, R precentral gyrus, R superior parietal gyrus, R middle temporal gyrus, and R cerebellum. The seed regions, left and right SMA from the AAL atlas, were also included (gold orbs). Although no significant expertise-related differences survived a conservative FDR correction, several trends for significance are shown in Figure 8B (*) at uncorrected $P < 0.05$ levels within our sample size of only 13 experts and 24 novices. Experts exhibited uncorrected higher numbers of connections than novices between R superior frontal gyrus and L posterior cingulate ($t = 2.10$, $P = 0.043$), R inferior frontal gyrus and R cerebellum ($t = 2.19$, $P = 0.035$), and R precentral gyrus, and both L posterior cingulate ($t = 3.09$, $P = 0.004$) and L insula ($t = 2.38$, $P = 0.023$). Novices exhibited higher numbers of connections than experts between R SMA and R inferior frontal gyrus ($t = -2.29$, $P = 0.028$), and L superior frontal gyrus and L insula ($t = -2.69$, $P = 0.011$).

DISCUSSION

In this article, we studied post-task resting state functional brain dynamics to examine their purported role in learning a recently performed task as a concomitant process in expertise development. Instead of using a conventional laboratory task and monetary incentives, we recruited athletes to perform a surrogate sports task in the laboratory, enabling a study of post-task resting state dynamics in a population with substantial expertise and intrinsic motivation for the task domain. We collected simultaneous fMRI/EEG data from Division 1 collegiate baseball players and age-matched controls with no baseball experience and conducted a seed-based connectivity analysis from L and R SMA regions defined from both fMRI voxels and EEG estimated sources to investigate functional relationships with performance-dependent BOLD signal fluctuations in non-SMA voxels. Our results highlight four main expertise differences: (1) experts had

TABLE III. Simultaneous fMRI/EEG Beta Power: Seed-based post-task resting state functional connectivity of EEG beta power using R and L SMA sources with all fMRI gray matter voxels outside of R and L SMA

Seed	Contrast	Region name	MNI coordinates			Voxels	*T*-score	*Z*-score
			X	*Y*	*Z*			
EEG beta power at R. SMA	**Experts > Non-experts**	(None)						
Controlling for fMRI signal at R. SMA	**Non-experts > Experts**	L superior frontal gyrus	−16	26	58	201	4.52	4.00
EEG Beta power at L. SMA	**Experts > Non-experts**	(None)						
Controlling for fMRI signal at L. SMA	**Non-experts > Experts**	L superior frontal gyrus	−18	26	60	302	4.99	4.32
		L cingulum posterior	−8	−42	10	239	3.82	3.47
EEG Beta power at R. SMA	**No-Go Accuracy regressor** *Controlling for expertise Positive Correlations*	R para-hippocampal gyrus	38	−38	−6	243	5.06	4.35
Controlling for fMRI signal at R. SMA								
	No-Go Accuracy regressor	L anterior cingulate cortex	−10	40	12	170	4.67	4.09
	Controlling for expertise Negative Correlations	L superior frontal gyrus	−6	32	56	287	4.32	3.84
EEG Beta power at L. SMA	**No-Go Accuracy regressor**	(None)						
Controlling for fMRI signal at L. SMA	*Controlling for expertise Negative/Positive Correlations*							

increased connectivity between bilateral SMA regions, including the preSMA, and L insula that may reflect expertise-level differences in post-task rumination critical for motor learning compared with controls, (2) differences in BOLD-alpha power correlations between groups, indicative of variability in modulatory attention in the post-task state and trained learning effects on connecting motor areas, (3) group differences between BOLD-beta power indicating possible expertise-level differences in cognitive processing of motor inhibition, and (4) we identified trends for several expertise-level differences in indirect structural connections that support functional connectivity network with SMA regions.

Group Differences in Motor Learning

Our seed connectivity analysis focused on whole-brain relationships with L and R SMA regions based on their known role in motor learning [Aizawa et al., 1991; Halsband and Freund, 1990; Halsband and Lange, 2006; Sakai et al., 1996] and from our previous experiments showing that activation of SMA regions during a Go/No-Go task could potentially be a marker of baseball expertise [Muraskin et al., in press; Muraskin et al., 2015]. Here, in our group functional connectivity analysis that examined expert versus control differences, we found that baseball experts have significantly greater functional connectivity between L and R SMA regions and L insula in the post-task resting state compared with controls. Although the insula is not typically thought of as a motor learning region, recent evidence has identified differential activity of L insula based on expertise or prior experience in a given field. A walking study compared highly fit people with those having poor fitness and found that the highly fit people (i.e., a type of expert group) had more insular activation during motor imagery [Godde and Voelcker-Rehage, 2010], indicating a role of the insula in motor circuits. A study with musicians found increased activity in L insula that was higher when musicians listened to a piece that they had previously rehearsed compared with a piece that they had never heard before, and this suggests that L insula is particularly important in learning when a person has prior experience in a certain field [Chein and Schneider, 2005]. Finally, research on error processing in Go/No-Go tasks [Hester et al., 2004; Menon et al., 2001] has found activation in bilateral insula, and this activity may lead to motor learning since effective motor circuits are key to performance on this task. Insula activity is also demonstrated during error processing in general [Bossaerts, 2010; Preuschoff et al., 2008; Ullsperger et al., 2010], which may reflect the region's more general role in learning by guiding a person to recognize, and ultimately avoid making a specific error in the future. Our results align with this previous research and suggest an additional role for functional connectivity between SMA and insula in expert motor learning during a post-task resting state. Since the post-task resting state represents a "task-driven" state of learning [Albert et al., 2009; Lewis et al., 2009; Vincent, 2009] and cognition [Grigg and Grady, 2010; Hasson et al., 2009; Waites et al., 2005], these differences in functional connectivity between experts and controls may represent different motor learning circuits in these two groups.

In our second group GLM analysis, we examined connectivity relationships with overall accuracy on the Go/

No-Go task while controlling for expertise, and we found that subjects who performed better on the task had significantly higher functional connectivity between L and R SMA and right-lateralized regions (specifically, R insula, R hippocampus, and R superior frontal gyrus) in the post-task resting state. This right lateralization was a bit unexpected since previous research has shown that the left hemisphere plays a larger role in motor learning circuits [Garry et al., 2004; Mutha et al., 2012; Suzuki et al., 2013]; however, a review article identified differential roles for the left and right hemispheres in motor learning [Halsband and Lange, 2006]. The literature review suggests that right hemisphere motor regions have strong activation during the early phases of motor learning while activation in the left hemisphere motor regions increases with practice and may serve as the storehouse for visuo-motor skills once mastered. Our group differences support this differential role for hemisphere specialization. The high task performers (when controlling for expertise) have right hemisphere involvement in the post-task resting state, which may reflect motor learning, while experts have a left hemisphere dominance that may capture their expertise and stored visuo-motor knowledge from extended practice.

Expertise effects in motor learning were also revealed in alpha power-BOLD correlations between motor regions and cerebellum. Recently, Mehrkanoon et al. [2016] used a motor learning task with EEG to perform a functional connectivity analysis on cortical sources. They showed that increases in functional connectivity between motor regions and cerebellum in the alpha band after motor learning. Our results show that experts have an increase in functional connectivity in the alpha band between SMA and cerebellum and which may be due to long-term motor training in experts.

Group Differences in Post-Task Attention Modulation

In addition to identifying group differences in motor learning, our finding that baseball experts have greater connectivity between bilateral SMA and L insula may reflect differences in attention modulation, a mechanism which supports motor learning circuits critical for expertise development [Jueptner et al., 1997; Stefan et al., 2004; Wulf, 2007; Wulf et al., 2001]. In meditation studies, expert meditators have consistently higher activation in L insula compared with novices, and researchers have suggested that this may reflect expert versus non-expert differences in the recruitment of attention-related neural resources [Lutz et al., 2013; Manna et al., 2010]. Since selective attention is important for implicit learning [Jiang and Chun, 2001], and similar brain regions are activated in implicit and explicit learning [Willingham et al., 2002], modulation of attention may indicate a mechanism by which motor

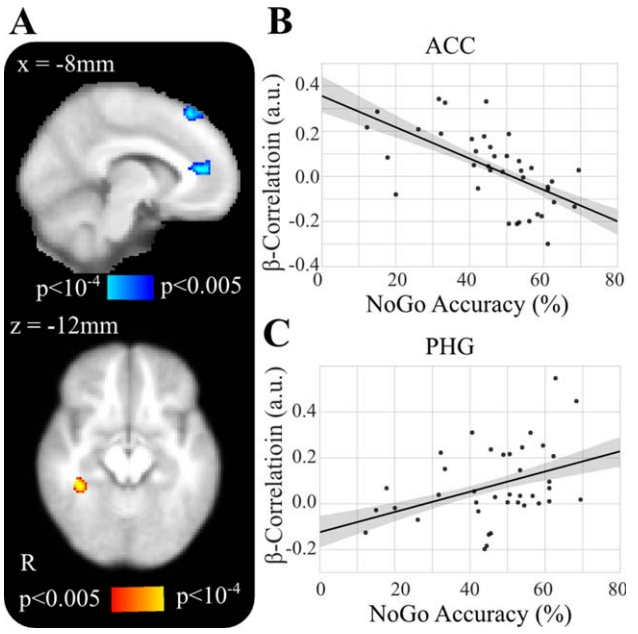

Figure 7.

R SMA β functional connectivity correlates with task performance. A, Overlay of significant clusters where No-Go task performance correlates with β-power to R SMA. B, Scatter plot of the β correlations from R SMA to ACC by the No-Go trial behavioral accuracy of each subject controlling for expertise. C, Scatter plot of the β correlations from R SMA to R parahippocampal gyrus by the No-Go trial behavioral accuracy of each subject controlling for expertise. [Color figure can be viewed at wileyonlinelibrary.com]

learning occurs during the post-task resting state scan in baseball experts.

Our SMA alpha analysis provides complementary support for this underlying attentional mechanism. In experts, there is a negative relationship between EEG alpha power at bilateral SMA and fMRI BOLD signal in L insula, indicating decreased insular activity with increased task performance, while there is only a negligible (close to 0) relationship for control participants. Given the role of EEG alpha oscillations in attention [Laufs et al., 2003a,; Ray and Cole, 1985] and inhibitory processes [Jensen and Mazaheri, 2010; Klimesch et al., 2007], our findings suggest that a neural circuit between bilateral SMA and L insula that is reliant on alpha band activity may have a role in modulation of attention, and it is well known that attention modulation is important for motor learning to occur [Jueptner et al., 1997; Stefan et al., 2004; Wulf, 2007; Wulf et al., 2001]. Taken together, we conclude that the higher bilateral SMA–L insula BOLD connectivity and stronger inverse correlation between SMA alpha power and L insula in experts likely reflect differential involvement of attention circuits in experts and controls in the post-task resting state, and these differences may facilitate enhancements in motor learning that are critical for expertise development.

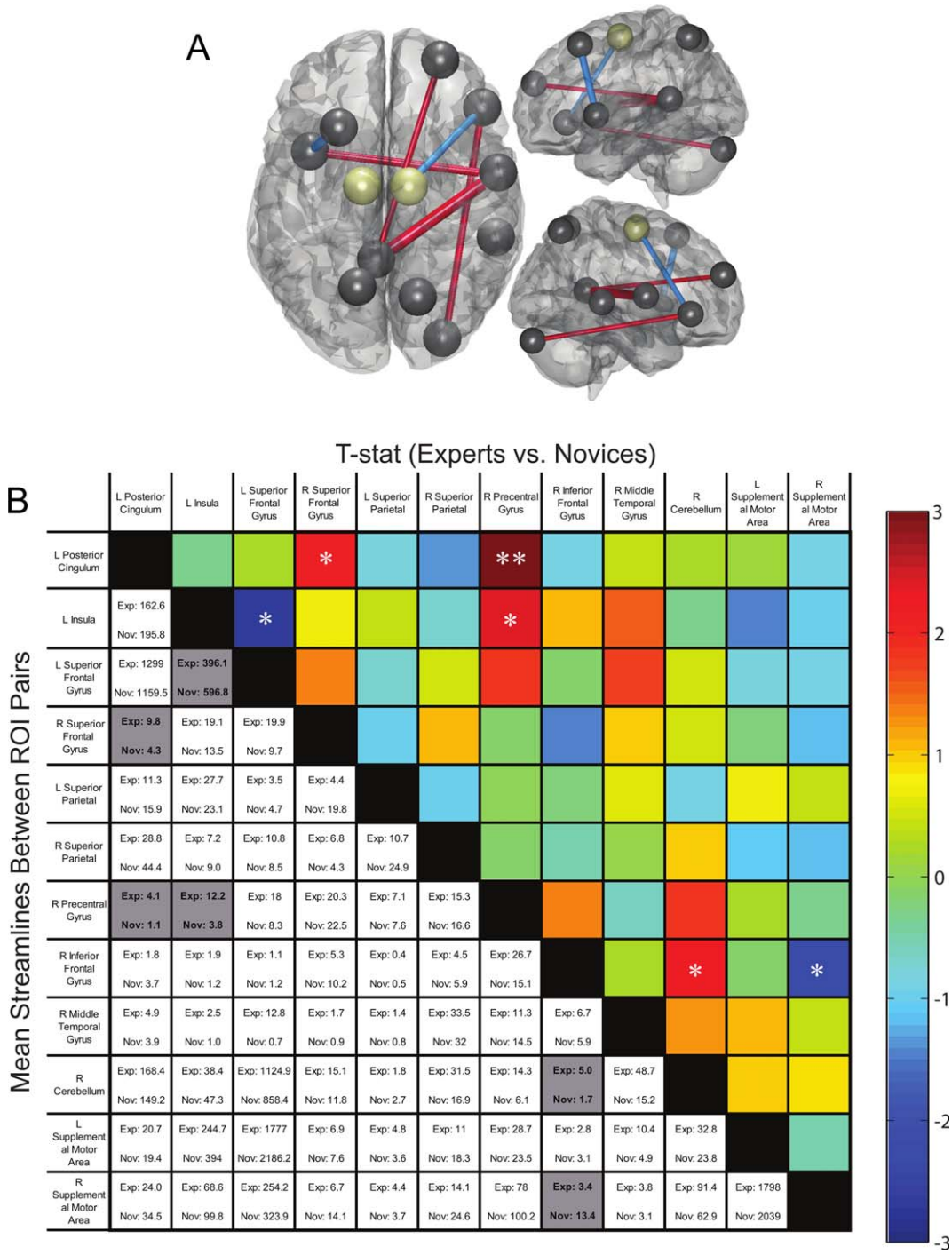

Figure 8.

Expert versus control structural differences. A, Black orbs are shown for all 10 functionally derived regions, and gold orbs for seed regions, that were included in the ROI analysis. Red connections indicate region pairs with higher streamline counts in experts while blue connections indicate higher streamline counts in novices. B, Mean numbers of streamlines (bottom left) with a color-scaled t-score map (top right) for streamline counts traversing between each region pair in experts and novices. Region pairs that have significant group differences ($P < 0.05$ uncorrected) are highlighted in gray or marked with an asterisk (*). While no correlations survived FDR correction, the ** cell trended toward significance. [Color figure can be viewed at wileyonlinelibrary.com]

Fronto-parietal brain regions have been implicated in attention [Coull et al., 1996; Naghavi and Nyberg, 2005], spatial attention deployment [Praamstra et al., 2005], and motor learning [Halsband and Lange, 2006]. These regions are recruited in a variety of contexts and tasks, including spatial and action perception [Matelli and Luppino, 2001], action observation [Buccino et al., 2001], action imagination [Johnson et al., 2002], and listening to motor sequences [Tettamanti et al., 2005]. A previous fMRI/EEG resting state study hypothesized that inverse correlations between alpha power and fMRI-BOLD signal in fronto-parietal brain regions reflect attention-modulatory circuits [Laufs et al., 2003b]. Our results support this hypothesis, revealing significant differences between experts and controls in the correlation between bilateral SMA alpha power and BOLD activity in bilateral fronto-parietal and primary motor regions. After post-hoc analyses, we found that these were inverse correlations in experts, but positive correlations in controls. These principles would suggest that in our study, some specific attention-related processes were occurring in the brains of expert baseball players who demonstrated inverse correlations in the post-task resting scan while controls had positive correlations between bilateral SMA alpha power and bilateral fronto-parietal and primary motor regions.

Group Differences in Post-Task Motor Inhibition

To examine the contribution of motor inhibition processes to expertise development in the post-task resting state scan, we investigated the relationship between fluctuations in BOLD activity and beta band activity from an EEG source located within SMA regions, including the preSMA, since several studies have found beta band involvement in motor response inhibition. In a Go/No-Go task, beta activity in macaques was found to have a significant rebound after desynchronization only after "No-Go" responses [Zhang et al., 2008], suggesting involvement of the beta band in response inhibition. Also, in a stop-signal task, an inhibitory beta band oscillation within a prefrontal–primary motor circuit was found during behavioral stopping [Swann et al., 2009]. Finally, our use of *a priori* ROI masks resulted in the SMA regional seed encompassing both SMA proper and the preSMA. The preSMA, particularly in the right hemisphere, is a critical part of the hyperdirect pathway that regulates reactive inhibition via communication with subcortical basal ganglia pathways [Aron et al., 2007; Aron and Poldrack, 2006; Dunovan et al., 2015]. In fact, the efficiency of communication between SMA regions, primarily the preSMA, and ventral lateral regions of the prefrontal cortex, including aspects of the insula reported in our functional network, have been shown to regulate the cortical control of proactive action inhibition like that required for successful completion in "No-Go" tasks [Aron, 2011].

Here, we compared experts and non-experts who performed well on "No-Go" trials to examine a similar inhibitory mechanism, and we found high accuracy on the "No-Go" trials had an inverse relationship between beta power in SMA regions and fMRI BOLD activity in a L prefrontal region and anterior cingulate cortex (ACC). That is, participants who successfully inhibited a response on the "No-Go" trials had decreased connectivity in the beta band between SMA regions and frontal regions. In addition, our post-hoc results found positive correlations between "No-Go" accuracy and R SMA beta power in the PHG. These results complement our previous finding that experts have more activity in occipital regions during inhibitory responses [Muraskin et al., 2015], and together, these studies provide evidence that occipital and motor regions are linked to SMA activity and that the strength of these connections can be a marker for accurate "No-Go" performance. The inverse relationship between SMA beta power and a L superior frontal region may reflect a process similar to the desynchronization of beta band oscillations that occurs during movement [Kuhn et al., 2004], and the positive correlations found in controls may reflect an idling motor cortex that is similar to the well-studied after-movement beta band synchronization [Pfurtscheller et al., 1998].

Group Differences in Structural Connectivity

The structural connectivity analysis provided additional insights into differences in functional networks between experts and controls. Using 10 functionally derived regions of interest from the fMRI/EEG analysis, we compared differences in the number of estimated fiber tracts between each pair of regions, where differences are interpreted as the strength of connection [Griffa et al., 2013]. Although the functional analysis identified these regions based on their connectivity relationships with SMA, we found no direct structural connections between SMA and regions that discriminated between experts and controls; however, there were several cases where several region pairs could account for observed functional relationships through indirect structural connections. For example, the SMA alpha functional connectivity relationship with the R cerebellum would potentially be mediated by structural connectivity between experts and novices in terms of structural connections from R SMA to R IFG, and then R IFG to R cerebellum (see Fig. 8). Future work may better elucidate the functional and structural networks that underlie brain dynamics of task experts, but our current results show that key parts of the functional network that differentiates experts from novices may arise in part from differences in the underlying structural connections.

Limitations

One limitation of the current methodology arises from the source localization technique used to identify the EEG time series in the SMA. Because of head volume

conduction, the estimated time series localized in an SMA source may have contributions from brain activity outside the region of interest. This is known as the "common feeding" problem for functional connectivity of EEG data, and several techniques using auto-regressive models and granger causality can untangle this issue in EEG connectivity analyses and identify if functional connectivity is directly between functional source A and B or whether the observed relationship between sources A and B originates from a common source C [Blinowska, 2011; Kaminski and Blinowska, 2014]. Since our methodology focused on connectivity in fMRI space, we did not assess evidence for a common EEG source, leaving open the possibility that brain areas outside of the SMA may contribute to the correlations seen in our alpha and beta frequency connectivity analyses. Future confirmatory studies may employ these complementary methods and examine the direct functional connectivity between pairs of cortical areas as power density and BOLD that account for this important "common feeding" issue.

An additional enhancement to our methodological approach could be individualization of the studied EEG frequency ranges. In our approach, the estimated SMA was computed separately for each participant to capture individual variability, but previous research has also shown that identifying individualized ranges for alpha and beta frequency ranges can improve overall signal-to-noise [Klimesch et al., 2007; Walz et al., 2015]. Individualized alpha/beta frequencies are often used when localizing sources in motor or occipital cortices due to empirical findings that these areas have large generators with highly individualized peak frequencies in the range of 8–12 Hz. However, relative to motor or occipital cortex, the power of these oscillations is significantly lower in the SMA, and it is difficult to identify specific frequencies on an individual subject basis in our targeted SMA seed regions. In our method, we increase the signal-to-noise ratio by estimating EEG alpha and beta sources in the SMA using common standard frequency bands across subjects, but this comes with the tradeoff of sacrificing individual subject specificity in the EEG source frequencies. Future research may address whether individualized frequency ranges further improves the relationship between brain and behavior.

Conclusion

This work investigated differences in the brain dynamics of the post-task resting state as a function of task expertise. We identified brain dynamics involving SMA regions showed expert-dependent differences underlying motor learning and cognitive task processing. We also found that expertise-related differences in structural connectivity could potentially account for some of the observed differences in the functional activity in the resting state. Though this work examined a specific population, namely baseball players, and created a surrogate task specific to their type of expertise, we believe that these findings would generalize to other populations where rapid perceptual decision making and enhanced perception-action coupling are critical for expertise.

ACKNOWLEDGMENTS

The views and conclusions contained in this document are those of the authors and should not be interpreted as representing the official policies, either expressed or implied, of the Army Research Laboratory or the U.S. Government. Authors Jordan Muraskin and Jason Sherwin are co-founders of deCervo, a private company that provides neuro-profiles for athletes. Author Timothy Verstynen has equity interest in Neuroscouting, a private company that provides services to baseball players.

REFERENCES

Adair RK (1990): The Physics of Baseball. New York: Harper & Row. 110 p.

Aizawa H, Inase M, Mushiake H, Shima K, Tanji J (1991): Reorganization of activity in the supplementary motor area associated with motor learning and functional recovery. Exp Brain Res 84:668–671.

Albert NB, Robertson EM, Miall RC (2009): The resting human brain and motor learning. Curr Biol: CB 19:1023–1027.

Armenti A (1992): The Physics of Sports. New York: American Institute of Physics.

Aron AR (2011): From reactive to proactive and selective control: Developing a richer model for stopping inappropriate responses. Biol Psychiatry 69:e55–e68.

Aron AR, Poldrack RA (2006): Cortical and subcortical contributions to Stop signal response inhibition: Role of the subthalamic nucleus. J Neurosci 26:2424–2433.

Aron AR, Durston S, Eagle DM, Logan GD, Stinear CM, Stuphorn V (2007): Converging evidence for a fronto-basal-ganglia network for inhibitory control of action and cognition. J Neurosci 27:11860–11864.

Behzadi Y, Restom K, Liau J, Liu TT (2007): A component based noise correction method (CompCor) for BOLD and perfusion based fMRI. NeuroImage 37:90–101.

Blinowska KJ (2011): Review of the methods of determination of directed connectivity from multichannel data. Med Biol Eng Comput 49:521–529.

Bossaerts P (2010): Risk and risk prediction error signals in anterior insula. Brain Struct Funct 214:645–653.

Brainard DH (1997): The psychophysics toolbox. Spatial Vision 10: 433–436.

Buccino G, Binkofski F, Fink GR, Fadiga L, Fogassi L, Gallese V, Seitz RdJ, Zilles K, Rizzolatti G, Freund HJ (2001): Action observation activates premotor and parietal areas in a somatotopic manner: An fMRI study. Eur J Neurosci 13:400–404.

Capotosto P, Babiloni C, Romani GL, Corbetta M (2009): Frontoparietal cortex controls spatial attention through modulation of anticipatory alpha rhythms. J Neurosci 29:5863–5872.

Cassim Fc, Monaca C, Szurhaj W, Bourriez JL, Defebvre L, Derambure P, Guieu JD (2001): Does post-movement beta synchronization reflect an idling motor cortex? Neuroreport 12:51.

Chein JM, Schneider W (2005): Neuroimaging studies of practice-related change: FMRI and meta-analytic evidence of a domain-

general control network for learning. Brain Res Cogn Brain Res 25:607–623.
Coull JT, Frith CD, Frackowiak RSJ, Grasby PM (1996): A fronto-parietal network for rapid visual information processing: A PET study of sustained attention and working memory. Neuropsychologia 34:1085–1095.
Dale AM (1999): Optimal experimental design for event-related fMRI. Hum Brain Mapp 8:109–114.
Delorme A, Makeig S (2004): EEGLAB: An open source toolbox for analysis of single-trial EEG dynamics including independent component analysis. J Neurosci Methods 134:9–21.
Dunovan K, Lynch B, Molesworth T, Verstynen T (2015): Competing basal ganglia pathways determine the difference between stopping and deciding not to go. Elife 4:08723.
Forstmann BU, Anwander A, Schafer A, Neumann J, Brown S, Wagenmakers EJ, Bogacz R, Turner R (2010): Cortico-striatal connections predict control over speed and accuracy in perceptual decision making. Proc Natl Acad Sci U S A 107:15916–15920.
Frank MJ, Gagne C, Nyhus E, Masters S, Wiecki TV, Cavanagh JF, Badre D (2015): fMRI and EEG predictors of dynamic decision parameters during human reinforcement learning. J Neurosci 35:485–494.
Garry MI, Kamen G, Nordstrom Ma (2004): Hemispheric differences in the relationship between corticomotor excitability changes following a fine-motor task and motor learning. J Neurophysiol 91:1570–1578.
Godde B, Voelcker-Rehage C (2010): More automation and less cognitive control of imagined walking movements in high- versus low-fit older adults. Front Aging Neurosci 2: 1–13.
Goldman RI, Wei CY, Philiastides MG, Gerson AD, Friedman D, Brown TR, Sajda P (2009): Single-trial discrimination for integrating simultaneous EEG and fMRI: Identifying cortical areas contributing to trial-to-trial variability in the auditory oddball task. NeuroImage 47:136–147.
Griffa A, Baumann PS, Thiran JP, Hagmann P (2013): Structural connectomics in brain diseases. NeuroImage 80:515–526.
Grigg O, Grady CL (2010): Task-related effects on the temporal and spatial dynamics of resting-state functional connectivity in the default network. PloS One 5:e13311.
Halsband U, Freund HJ (1990): Premotor cortex and conditional motor learning in man. Brain 113:207–222.
Halsband U, Lange RK (2006): Motor learning in man: A review of functional and clinical studies. J Physiol Paris 99:414–424.
Hari R, Salmelin R (1997): Human cortical oscillations: A neuromagnetic view through the skull. Trends Neurosci 20:44–49.
Hasson U, Nusbaum HC, Small SL (2009): Task-dependent organization of brain regions active during rest. Proc Natl Acad Sci U S A 106:10841–10846.
He B, Dai Y, Astolfi L, Babiloni F, Yuan H, Yang L (2011): eConnectome: A MATLAB toolbox for mapping and imaging of brain functional connectivity. J Neurosci Methods 195:261–269.
Heekeren HR, Marrett S, Bandettini Pa, Ungerleider LG (2004): A general mechanism for perceptual decision-making in the human brain. Nature 431:859–862.
Hester R, Fassbender C, Garavan H (2004): Individual differences in error processing: A review and reanalysis of three event-related fMRI studies using the GO/NOGO task. Cereb Cortex (New York, N.Y.: 1991) 14:986–994.
Hyvarinen A (1999): Fast and robust fixed-point algorithms for independent component analysis. IEEE Trans Neural Netw 10: 626–634.
Jahfari S, Verbruggen F, Frank MJ, Waldorp LJ, Colzato L, Ridderinkhof KR, Forstmann BU (2012): How preparation changes the need for top-down control of the basal ganglia when inhibiting premature actions. J Neurosci 32:10870–10878.
Jensen O, Mazaheri A (2010): Shaping functional architecture by oscillatory alpha activity: Gating by inhibition. Front Human Neurosci 4:186.
Jiang Y, Chun MM (2001): Selective attention modulates implicit learning. Q J Exp Psychol A, Hum Exp Psychol 54:1105–1124.
Johnson SH, Rotte M, Grafton ST, Hinrichs H, Gazzaniga MS, Heinze HJ (2002): Selective activation of a parietofrontal circuit during implicitly imagined prehension. NeuroImage 17:1693–1704.
Jueptner M, Stephan KM, Frith CD, Brooks DJ, Frackowiak RSJ, Passingham RE (1997): Anatomy of motor learning. I. Frontal cortex and attention to action. J Neurophysiol 77:1313–1324.
Kaminski M, Blinowska KJ (2014): Directed Transfer Function is not influenced by volume conduction-inexpedient pre-processing should be avoided. Front Comput Neurosci 8:61.
Klimesch W, Doppelmayr M, Russegger H, Pachinger T, Schwaiger J (1998): Induced alpha band power changes in the human EEG and attention. Neurosci Lett 244:73–76.
Klimesch W, Sauseng P, Hanslmayr S (2007): EEG alpha oscillations: The inhibition-timing hypothesis. Brain Res Rev 53: 63–88.
Kristeva-feige R, Fritsch C, Timmer J, Lu Ch (2002): Effects of attention and precision of exerted force on beta range EEG-EMG synchronization during a maintained motor contraction task. Clin Neurophysiol 113:124–131.
Kuhn AA, Williams D, Kupsch A, Limousin P, Hariz M, Schneider GH, Yarrow K, Brown P (2004): Event-related beta desynchronization in human subthalamic nucleus correlates with motor performance. Brain 127:735–746.
Laufs H, Kleinschmidt a, Beyerle a, Eger E, Salek-Haddadi a, Preibisch C, Krakow K (2003a): EEG-correlated fMRI of human alpha activity. NeuroImage 19:1463–1476.
Laufs H, Krakow K, Sterzer P, Eger E, Beyerle a, Salek-Haddadi a, Kleinschmidt a (2003b): Electroencephalographic signatures of attentional and cognitive default modes in spontaneous brain activity fluctuations at rest. Proc Natl Acad Sci U S A 100: 11053–11058.
Laufs H, Holt JL, Elfont R, Krams M, Paul JS, Krakow K, Kleinschmidt A (2006): Where the BOLD signal goes when alpha EEG leaves. NeuroImage 31:1408–1418.
Lewis CM, Baldassarre A, Committeri G, Luca G (2009): Learning sculpts the spontaneous activity of the resting human brain. Proc Natl Acad Sci U S A 106:17558.
Lutz A, McFarlin DR, Perlman DM, Salomons TV, Davidson RJ (2013): Altered anterior insula activation during anticipation and experience of painful stimuli in expert meditators. NeuroImage 64:538–546.
Manna A, Raffone A, Perrucci MG, Nardo D, Ferretti A, Tartaro A, Londei Aa (2010): Neural correlates of focused attention and cognitive monitoring in meditation. Brain Res Bull 82:46–56.
Matelli M, Luppino G (2001): Parietofrontal circuits for action and space perception in the macaque monkey. NeuroImage 14: S27–S32.
Mehrkanoon S, Boonstra TW, Breakspear M, Hinder M, Summers JJ (2016): Upregulation of cortico-cerebellar functional connectivity after motor learning. NeuroImage 128:252–256.
Menon V, Adleman NE, White CD, Glover GH, Reiss AL (2001): Error-related brain activation during a go nogo response inhibition task. Hum Brain Mapp 143:131–143.

Miura A, Nakata H, Kudo K, Yoshie M (2010): Characteristics of the athletes' brain: Evidence from neurophysiology and neuroimaging. Brain Res Rev 62:197–211.

Muraskin J, Sherwin J, Lieberman G, Garcia JO, Verstynen T, Vettel JM, Sajda P (in press) Fusing multiple neuroimaging modalities to assess group differences in perception-action coupling. Proceedings of the IEEE. doi: 10.1109/JPROC.2016.2574702

Muraskin J, Sherwin J, Sajda P (2015): Knowing when not to swing: EEG evidence that enhanced perception-action coupling underlies baseball batter expertise. NeuroImage 123: 1–10.

Mutha PK, Haaland KY, Sainburg RL (2012): the effects of brain lateralization on motor control and adaptation. J Motor Behav 44:455–469.

Naghavi HR, Nyberg L (2005): Common fronto-parietal activity in attention, memory, and consciousness: Shared demands on integration? Conscious Cogn 14:390–425.

Nakamoto H, Mori S (2008): Effects of stimulus-response compatibility in mediating expert performance in baseball players. Brain Res 1189:179–188.

Pelli DG (1997): The VideoToolbox software for visual psychophysics: Transforming numbers into movies. Spatial Vision 10: 437–442.

Pfurtscheller Ga (1996): Post-movement beta synchronization. A correlate of an idling motor area? Electroencephalogr Clin Neurophysiol 98:281–293.

Pfurtscheller G, Zalaudek K, Neuper C (1998): Event-related beta synchronization after wrist, finger and thumb movement. Electroencephalogr Clin Neurophysiol 109:154–160.

Praamstra P, Boutsen L, Humphreys GW (2005): Frontoparietal control of spatial attention and motor intention in human EEG. J Neurophysiol 94:764–774.

Preuschoff K, Quartz SR, Bossaerts P (2008): Human insula activation reflects risk prediction errors as well as risk. J Neurosci 28:2745–2752.

Radlo SJ, Janelle CM, Barba DA (2001): Perceptual decision making for baseball pitch recognition: Using P300 latency and amplitude to index attentional processing. Res Q Exerc Sport 72:22–31.

Ray WJ, Cole HW (1985): EEG alpha activity reflects attentional demands, and beta activity reflects emotional and cognitive processes. Science 228:750–752.

Sajda P, Goldman RI, Dyrholm M, Brown TR (2010): Signal Processing and Machine Learning for Single-Trial Analysis of Simultaneously Acquired EEG and fMRI. in Statistical Signal Processing for Neuroscience and Neurotechnology, Academic Press, Incorporated, pp. 311–334.

Sakai K, Miyauchi S, Sasaki Y, Putz B, Hikosaka O, Sakai K, Miyauchi S, Takino R, Sasaki Y, Putz B (1996): Activation of human presupplementary motor area in learning of sequential procedures: A functional MRI study. J Neurophysiol 76: 617–621.

Sherwin J, Sajda P (2013): Musical experts recruit action-related neural structures in harmonic anomaly detection: Evidence for embodied cognition in expertise. Brain Cogn 83: 190–202.

Sherwin J, Muraskin J, Sajda P (2012): You can't think and hit at the same time: Neural correlates of baseball pitch classification. Front Neurosci 6:177.

Sherwin JS, Muraskin J, Sajda P (2015): Pre-stimulus functional networks modulate task performance in time-pressured evidence gathering and decision-making. NeuroImage 111: 513–525.

Simmonds DJ, Pekar JJ, Mostofsky SH (2008): Meta-analysis of Go/No-go tasks demonstrating that fMRI activation associated with response inhibition is task-dependent. Neuropsychologia 46:224–232.

Stefan K, Wycislo M, Classen J (2004): Modulation of associative human motor cortical plasticity by attention. J Neurophysiol 92:66–72.

Suzuki T, Higashi T, Takagi M, Sugawara K (2013): Hemispheric asymmetry of ipsilateral motor cortex activation in motor skill learning. Neuroreport 24:693–697.

Swann N, Tandon N, Canolty R, Ellmore TM, McEvoy LK, Dreyer S, DiSano M, Aron AR (2009): Intracranial EEG reveals a time- and frequency-specific role for the right inferior frontal gyrus and primary motor cortex in stopping initiated responses. J Neurosci 29:12675–12685.

Tettamanti M, Buccino G, Saccuman MC, Gallese V, Danna M, Scifo P, Fazio F, Rizzolatti G, Cappa SF, Perani D (2005): Listening to action-related sentences activates fronto-parietal motor circuits. J Cogn Neurosci 17:273–281.

Tzourio-Mazoyer N, Landeau B, Papathanassiou D, Crivello F, Etard O, Delcroix N, Mazoyer B, Joliot M (2002): Automated anatomical labeling of activations in SPM using a macroscopic anatomical parcellation of the MNI MRI single-subject brain. NeuroImage 15:273–289.

Ullsperger M, Harsay Ha, Wessel JR, Ridderinkhof KR (2010): Conscious perception of errors and its relation to the anterior insula. Brain Struct Funct 214:629–643.

Vincent JL (2009): Learning and memory: While you rest, your brain keeps working. Curr Biol: CB 19:R484–R486.

Waites AB, Stanislavsky A, Abbott DF, Jackson GD (2005): Effect of prior cognitive state on resting state networks measured with functional connectivity. Hum Brain Mapp 24: 59–68.

Walz JM, Goldman RI, Carapezza M, Muraskin J, Brown TR, Sajda P (2013): Simultaneous EEG-fMRI reveals temporal evolution of coupling between supramodal cortical attention networks and the brainstem. J Neurosci 33: 19212–19222.

Walz JM, Goldman RI, Carapezza M, Muraskin J, Brown TR, Sajda P (2015): Prestimulus EEG alpha oscillations modulate task-related fMRI BOLD responses to auditory stimuli. NeuroImage 113:153–163.

Wang Z, Liu J, Zhong N, Qin Y, Zhou H, Li K (2012): Changes in the brain intrinsic organization in both on-task state and post-task resting state. NeuroImage 62:394–407.

Wang Y, Zhang X, Huang J, Zhu M, Guan Q, Liu C (2013): Associations between EEG beta power abnormality and diagnosis in cognitive impairment post cerebral infarcts. J Mol Neurosci: MN 49:632–638.

Whitfield-Gabrieli S, Nieto-Castanon A (2012): Conn: A functional connectivity toolbox for correlated and anticorrelated brain networks. Brain Connect 2:125–141.

Willingham DB, Salidis J, Gabrieli JDE (2002): Direct comparison of neural systems mediating conscious and unconscious skill learning. J Neurophysiol 88:1451–1460.

Wulf G (2007): Attentional focus and motor learning: A review of 10 years of research. E-journal Bewegung Train 1: 1–11.

Wulf G, Prinz W, Planck M (2001): Directing attention to movement effects enhances learning: A review. Psychon Bull Rev 8: 648–660.

Yeh FC, Tseng WY (2011): NTU-90: a high angular resolution brain atlas constructed by q-space diffeomorphic reconstruction. NeuroImage 58:91–99.

Yeh FC, Verstynen TD, Wang Y, Fernandez-Miranda JC, Tseng WY (2013): Deterministic diffusion fiber tracking improved by quantitative anisotropy. PloS One 8:e80713.

Zhang Y, Chen Y, Bressler SL, Ding M (2008): Response preparation and inhibition: The role of the cortical sensorimotor beta rhythm. Neuroscience 156:238–246.

Zhang S, Ide JS, Li CS (2012): Resting-state functional connectivity of the medial superior frontal cortex. Cereb Cortex 22: 99–111.

Zhang H, Long Z, Ge R, Xu L, Jin Z, Yao L, Liu Y (2014): Motor imagery learning modulates functional connectivity of multiple brain systems in resting state. PloS One 9:e85489.